JOURNAL OF SPACECRAFT AND ROCKETS
Vol. 29, No. 4, July-August 1992

Magnetospheric Ion Composition Spectrometer Onboard the CRRES Spacecraft

B. Wilken* and W. Weiß†
Max-Planck-Institut für Aeronomie, 3411 Katlenburg-Lindau, Germany
D. Hall‡ and M. Grande§
Rutherford-Appleton Laboratories, Chilton, Didcot, Oxfordshire OX11 OQX, England, United Kingdom
F. Søraas¶
University of Bergen, 5014 Bergen-U, Norway
and
J. F. Fennell*
The Aerospace Corporation, Los Angeles, California 90009

The magnetospheric ion composition spectrometer (MICS) in the CRRES scientific payload utilizes time-of-flight and energy spectroscopy in combination with an electrostatic entrance filter to measure the mass A, energy E, and ionic charge Q of particles with energies between 1 keV/charge and 430 keV/charge. An advanced ogive design of the electrostatic filter system provides a narrow angle of acceptance and high sensitivity. Incident particles are postaccelerated prior to entering the detection segment in order to improve the resolution at the lower end of the useful energy range. The principle features of the MICS spectrometer are described in some detail. Selected data gathered in-flight are shown as an illustration of the instrument performance in the operational orbit.

I. Introduction

THE magnetospheric ion composition spectrometer (MICS) in the payload of the Combined Release and Radiation Effects Satellite (CRRES) belongs to a class of advanced instruments which provide full characterization of incident ions by determining their mass A (in amu), charge Q, and velocity V (magnitude and direction) as independent parameters. The particle's identity is derived from a time-of-flight T and energy E measurement, and the ionic charge Q is obtained from an electrostatic energy per charge E/Q filter which serves as the entry element of the spectrometer. Upon leaving the E/Q filter the ion's energy is increased by a post-accelerating voltage to improve the instrument resolution at low particle energies.

The MICS energy range extends from 1.2 keV/charge up to 426.5 keV/charge, and ion species are identified from hydrogen to iron. The obtainable mass resolution $A/\mathrm{d}A$ is a complex function of the particle mass and energy. For a given ion species the mass resolution increases as a function of the energy per mass ratio E/A. A typical ratio $A/\mathrm{d}A = 8$ is obtained for oxygen ions with energies above 100 keV. Despite this only moderate mass resolution, atoms and molecules, even isobaric structures, can be discriminated by a peculiarity of the MICS detection technique: Fragmentation of swift molecules in the thin START foil of the T/E spectrometer leads to groups of particles which travel with the original velocity but each fragment's energy is apportioned to its mass. The resulting statistical distribution in (E, T) space can be used to identify the presence of molecules.

The general principles of the particle identification techniques employed in MICS are well established (compare, e.g., Ref. 1 and references therein) and design concepts for major elements such as the time-of-flight detector and the associated analog electronics [herein referred to as signal conditioning unit (SCU)] have strong lines of heritage to similar ion-mass spectrometers flown successfully on AMPTE, VIKING, ULYSSES, and GIOTTO.

The MICS spectrometer emerged from a concept originally conceived for the CAMMICE instrument package that was submitted to and selected by NASA for inclusion in the Global Geospace Science (GGS) mission elements EQUATOR and POLAR. Programmatic problems forced NASA to modify and delay GGS. In 1980, the MICS spectrometer was accepted for the Swedish national satellite VIKING and returned valuable scientific data throughout the operational life of the satellite (Feb. 1986 to May 1987).

The MICS/VIKING experimenter team proposed a similar instrument with added postacceleration for the CRRES mission. Design and implementation of MICS/CRRES is a good example for international cooperation in a low-budget/no management environment.

MICS is using an unusual electrostatic filter design which combines a rather good definition of the incident particle direction (narrow acceptance angle) with high detection sensitivity (large acceptance area). The instrument's conceptually small angular cone in velocity space samples the pitch-angle (PA) distribution of the energetic particle population with high angular resolution as the spacecraft rotates about its spin axis.

II. Scientific Objectives

The MICS instrument not only measures dynamic quantities (vector velocity and energy) but also characterizes completely the particle's nature (ionic charge Q and nuclear mass A). In the CRRES orbit, MICS is an important tool to determine the plasma composition over an extended energy range and to measure the pitch-angle distribution of the individual plasma component with high resolution. The accepted energy range (1.2-436 keV/e) covers the relevant regime of the plasma

Received July 9, 1991; revision received April 9, 1992; accepted for publication April 13, 1992.

*Senior Scientist.
†Senior Engineer.
‡Group Leader.
§Instrument Manager.
¶Professor.

distribution functions in the ring current and the outer magnetosphere.

The viewing direction of MICS in the spacecraft frame is illustrated in Fig. 1. The orbital attitude of CRRES implies that the narrow field of view (± 1.1 deg) samples PA distributions essentially in the $(YZ)_{GSE}$ plane as the spacecraft rotates about its sun pointing spin axis. Under nominal magnetospheric conditions, the magnetic field vector is close to or in the $(YZ)_{GSE}$ plane, and thus MICS determines spherical PA functions over the entire range in polar angle in a fixed azimuthal plane. The determination of distribution functions for different ion species (A, Q) is the prime objective of MICS although, in general, isotropy in the azimuthal angle has to be assumed. The good mass and charge resolution allows studies of temporal variations in these particle parameters. The evolution of the plasma composition under dynamic conditions sheds light not only on the nature of energization processes in the magnetosphere but also on the coupling of turbulences to the ionosphere and solar wind as the dominant plasma sources.

The chemical release campaigns at high altitudes are a second major field of interest. It is unlikely that MICS will respond to the injected nuclei before substantial acceleration has occurred. However, the explosive releases in a distance of a few kilometers from the spacecraft create plasma effects which propagate away from the localized injection site and reach the CRRES position within a few seconds. This was indeed confirmed by the barium releases in January 1991.

III. Ion Identifying Technique

The detection technique in the MICS ion spectrometer is based on a particle identifying function obtained from a combined time-of-flight T and energy E measurement: The ion mass A is proportional to the quantity $E \cdot T^2$. Addition of an electrostatic filter (ESA), which accepts only particles with a defined energy per charge E/Q ratio, allows the determination of the ionic charge Q. To improve the sensitivity and charge resolution of the instrument at low particle energies, a postaccelerating voltage U is applied between the ESA and the T/E detector system. The observed particle energy E is then $E = E_0 + UQ = Q[(E_0/Q) + U]$ with E_0 denoting the incident particle energy. This clearly shows the advantage of postacceleration for particles with small E_0/Q values.

Functionally, the MICS spectrometer is composed of the sensor system and the digital processing unit (DPU) which actually form two physically separated mechanical structures. The "sensor system" represents the front end of the spectrometer comprising the particle detectors and the analog electronics including the signal shaping and control logic (as mentioned earlier this subsystem is called the signal conditioning unit or SCU). Major elements of the sensor system are as follows:

1) The toroidal electrostatic analyzer (ESA) with integrated high-voltage generators (variable deflection voltage and postaccelerating voltage).

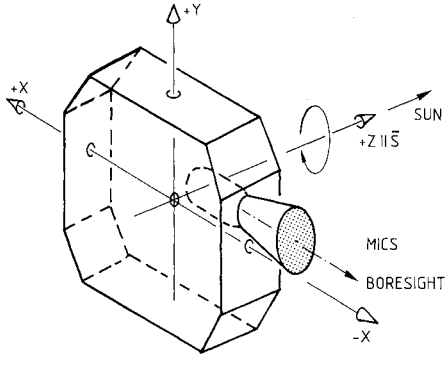

Fig. 1 Orientation and look direction of the MICS ion composition spectrometer.

Table 1 Selected parameters of the MICS sensor system

Energy range, keV/e	1.2–426.5
Mass range, amu	1–50
Mass resolution, A/dA	8 (A = 16)
Weight, kg	4.5
Power, W	3.6

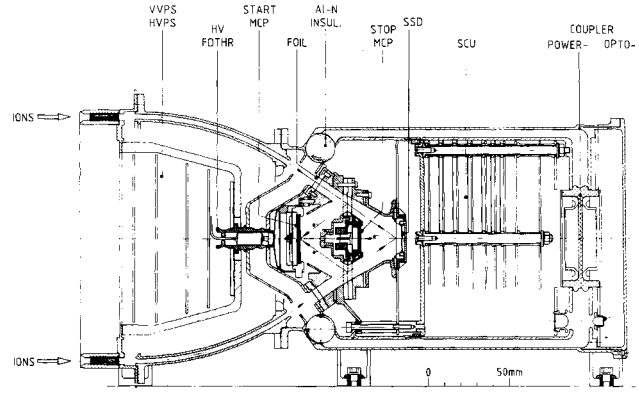

Fig. 2 Scaled cross section of the MICS sensor system.

2) The time-of-flight/energy sensor system and the follow-on signal conditioning unit (SCU). These components are contained in an electrically isolated "Faraday cage" called the high-potential "bubble." The inner surface of the bubble is held at the high (negative) potential of the accelerating voltage.

3) The power and signal coupling system which connects the bubble electronics to ground potential, i.e., to the DPU input circuitry and power supplies.

The electronic signals generated in the "sensor system" are transferred to the DPU subsystem for evaluation and preparation for the telemetry system. The DPU preprocesses the particle data and extracts relevant parameters, the DPU also is in complete command of the SCU by continuously refreshing the contents of the status registers in the high-voltage bubble. Some technical and physical parameters of the MICS sensor system are summarized in Table 1.

The following sections delineate functional principles of major MICS components in detail. Initial results from in-orbit observations are presented to illustrate the potential of the spectrometer.

A. MICS Sensor System

The scaled cross section in Fig. 2 shows the essential elements of the MICS sensor system: ESA, the concentric dual bubble concept, the T/E detector system and SCU assembled in the inner high potential bubble, and the power/signal coupler system. As mentioned previously, the SCU accepts the detector output signals, provides amplification and proper signal conditioning, and converts the E- and T- signal amplitudes into binary codes prior to transmission across the potential barrier. The scientific data (coded amplitude information and related counting rates formed in the SCU) are transmitted via opto-couplers to the DPU for further evaluation and for interfacing with the telemetry system (principle functions of the DPU are discussed in Sec. III.B). Generally speaking, the division line between SCU and DPU is somewhat arbitrary. However, operation of a T/E detector system in a high-voltage bubble clearly favors a functional interface with all-digital communication lines.

Application of postacceleration requires to float the inner bubble with the T/E detector system and the SCU at a high potential. A four-point support system is employed to translate the mechanical forces to the inner bubble and to provide

electric isolation: Three spherical standoffs at the front side, made from highly isolating but heat conducting Al-N ceramic material, and a single Vespel element with the power coupler (described in Sec. III.A.4) at the back side, suspend the high-potential bubble inside the grounded outer structure.

The dual concentric bubble design is an important feature of the MICS high-voltage system: the postaccelerating electric field is completely confined to the vacuum gap between the outer and inner bubbles. The field distribution in the gap is mostly homogeneous and critical fieldline concentrations are avoided except for areas where insulators bridge the vacuum gap.

1. Electrostatic Analyzer and the High-Voltage Power Supplies (VVPS and HVPS)

The magnetospheric applications of MICS require an ESA design with good angular resolution and large geometric factor for the detection of heavy ions. Furthermore, the ion optics of the analyzer should be consistent with the geometry of a powerful T/E detector system On the basis of these requirements, an ogive design was chosen for the MICS spectrometer (compare Gough[2]).

The deflecting plates of the analyzer are surfaces of rotation, of circular axial profile. The generating ogives have radii of 166.5 and 169.5 mm. An ion of appropriate energy-to-charge ratio E/Q entering the analyzer is deflected through an angle of 35 deg on a circular track with a median radius of 168 mm (compare Fig. 2).

The ESA opening aperture is an annulus of inner radius 74.5 mm and outer radius 77.5 mm. Prior to entering the gap between the deflecting plates, incident ions pass through a collimating entry element which matches the analyzer opening. The purpose of this collimator is to reduce scattering inside the ESA and to suppress particles with oblique trajectories. The annular collimator consists of 140 stainless-steel grids, of hexagonal design, each pore having an open width of 0.7 mm. The stacked grids form a multichannel collimator with a narrow field-of-view and large open area. The collimation half-angle of the 0.7 by 18 mm channels is 2.2 deg and the total aperture of the collimator is 0.07 cm^2 sr.

After passing through the analyzer, the ion enters the post-acceleration region to increase its energy for improved energy and charge. The geometry and structure of the accelerating field means that special measures are not necessary to suppress photoelectrons. The detailed design of the field in this transfer region is the result of numerical modeling. A schematic representation of the analyzer/detector geometry is given in Fig. 3. Relevant parameters are summarized in Table 2.

The high-voltage power supplies (VVPS and HVPS) are integrated into the inner ogive. As well as being very volume efficient, this arrangement gives the control electronics an extra degree of radiation protection. The HV supplies consist of three PC-boards, a common control board, and two high-voltage generators. The (negative) swept high-voltage generator (VVPS), which is connected to the inner surface of the

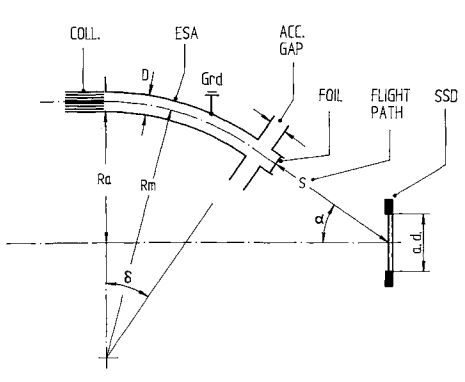

Fig. 3 Principle geometry of the ogive analyzer/detector assembly.

Table 2 Physical parameters of the ESA and the T-E detector system

ESA	
Collimation angle	± 1.1 deg
Collimator radius R_a, mm	74.5
Radius of curvature R_m, mm	168
Gap D, mm	3.0
Bending angle δ	35 deg
Analyzer constant	30.8
Bandwidth $\Delta E/E$	10%
Sensitivity, $cm^2 \cdot sr \cdot keV$	4.4×10^{-3}
T/E detector	
Flightpath s, mm	63.5
Cone angle α	33.5 deg
SSD diameter, mm	16

analyzer, uses a single transistor oscillator to step up the voltage, giving good efficiency and cool transformer running. An 11-stage voltage multiplier is used. The HVPS, which supplies the postacceleration voltage, is basically very similar but has slightly different values on some components and a 12-stage multiplier. In both cases, the current in the feedback resistor is monitored and compared to a reference.

The VVPS has 32 programmable levels, logarithmically spaced with a ratio of 1.31 for the lower 16 levels and 1.117 for the upper levels, with a top voltage of 14.4 kV. This leads to an energy range from 1.2–427 keV/charge, each step having a bandpass of 10%. The HVPS voltage is programmable in eight equal steps between 7.6–24.5 kV.

2. Time-of-Flight and Energy Detector

As shown in Fig. 2, ions leaving the analyzer travel on converging trajectories with an apex on the ESA's axis of rotation. The conical T/E detector system is perfectly adapted to this focussing feature of the ion optics. The entry element of the time (T) measuring system is a thin carbon foil (typically 5 $\mu g/cm^2$) on a conical surface which matches the annular exit slit of the ESA. Swift particles passing through the foil lead to the ejection of secondary electrons (SE) from the foil surface. The SE are accelerated to 1 keV. A conical electrostatic reflector collects the electrons on a microchannel plate (START MCP in Fig. 2). The MCP output signal serves as the START signal for the time-of-flight measurement. After traversing the flight path s the particle delivers its residual energy to the solid-state detector (SSD) mounted in the ESA apex. Again a small fraction of the particle energy is converted to SEs which escape from the SSD surface. These electrons are transferred to a second MCP detector (Fig. 2) to provide the STOP signal for the T measurement. The output signals from the microchannel plates (START and STOP) and the SSD (energy E) represent the analog input information for the SCU. Principle dimensions of the T/E detector configuration are given in Table 2.

3. Signal Conditioning Unit

The SCU configures the spectrometer system, accepts detector signals, and transfers the latter to the DPU. A simplified block diagram of the SCU in the high-voltage bubble, including the signal and power couplers, is presented in Fig. 4. Concept and technique of the SCU and coupler design was strongly guided by following considerations or preferences: 1) The power consumption and weight has to be kept at a minimum; and 2) The radiation tolerance must exceed 100 krad. These two requirements have considerable impact on the choice of parts and components in particular for the high-frequency circuitry required for the time-of-flight segment. Conceptually, the SCU design was driven by the following ideas:

1) The SCU has no autonomous function; i.e., the SCU is at all times under complete control of the DPU.

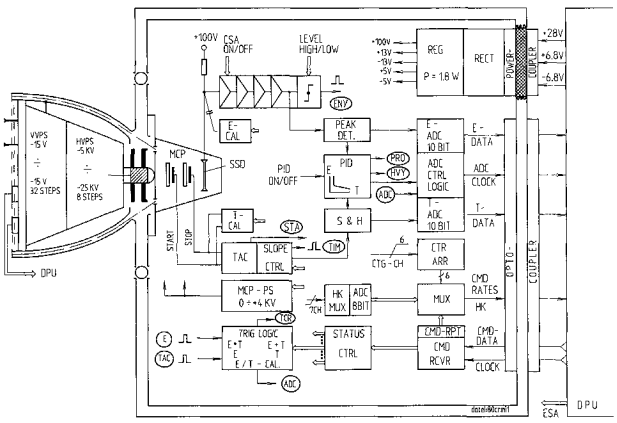

Fig. 4 Simplified block diagram of the SCU.

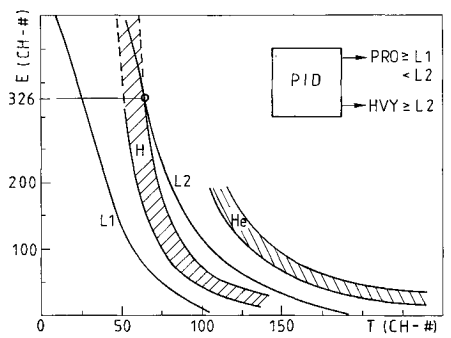

Fig. 5 Measured loci for hydrogen and helium ions in energy-time space.

2) Communication across the potential barrier uses digital signals only. Serial transmission for each data category leads to a small number of signal lines.

3) The electrostatic layout of the data and power couplers must comply with the general concept of the high-voltage system; i.e., the isopotential surfaces of the inner and outer bubble should be continuous through the coupler.

Event logic and analog particle identifier. As shown in Fig. 4, the analog energy signals created in the SSD are passed through a shaping amplifier chain and stored in a peak detector (PEAK DET) for subsequent digitization in a 10-bit ADC (E-ADC). In the time channel, a time-to-amplitude converter (TAC) generates an analog signal amplitude proportional to the time interval between START and STOP pulses. A sample-and-hold circuit (S & H) stores the signal sufficiently long to allow digitization in a 10-bit converter (T-ADC).

The binary T and E data are transmitted to ground potential via two opto-couplers. The conversion process in the dual E/T-ADC system is controlled by the ADC logic (ADC CTRL LOG) which receives input functions from the particle identifier (PID) and the trigger logic (TRIG LOG). In fact, the trigger logic (TRIG LOG) defines the nature of observed events according to the logic condition selected by the DPU. It is important, however, to note that the PID can effect the observed counting rates. For the PID OFF situation, TRIG LOG can set the following conditions:

1) *Logic:* $E \cdot T$. Events with coincident E and T signals. Either type of signal can start the 1.2-μs event window, but the event is processed only if the second signal arrives within the window.

2) *Logic:* $E + T$. Events with valid E or T signals. Either type of signal can start the 1.2 μs event window and the event is processed irrespective of the presence of the second signal.

3) *Logic:* E. Events with valid E signals (T signal is not required). Dead time: 1.2 μs.

4) *Logic:* T. Events with valid T signals (E signal is not required). Dead time: 1.2 μs.

The chosen trigger condition has obviously great significance for the MICS detection efficiency because of the physics involved in the particle detection process and its statistical nature. Trigger condition 1 selects events with coincident (E,T) signals which provides the cleanest definition of a particle. However, such an event pattern has the lowest occurrence probability due to fluctuations in the signal formation and is, furthermore, rather susceptible to anomalies in the E and T analog channels. Trigger condition 2 is obviously the most universal one which accepts all possible event types (E,T; $0,T$; $E,0$). This condition is therefore considered the baseline for routine in-orbit operations. Conditions 3 and 4 allow elimination of one of the two analog channels. These options will be exercised only if drastic deterioration in the detector performance make conditions 1 and 2 obsolete. Relevant SCU parameters are shown in Table 3.

The analog E and T amplitudes are not only sent to the dual ADC system but also to the PID which is a fast analog processor evaluating the analog (E,T) information. The digitization process in the ADCs will be interrupted and a reset signal issued if PID detects a proton event. The PID decision time is 1.5 μs.

The main purpose of the PID is to prevent high proton fluxes from overloading the relatively slow analog-to-digital conversion. The ADC (E and T) dead time is set to $t = 42$ μs to match the transmission rate of the opto-couplers. The PID circuit reduces the effective dead time for proton detection to 1.5 μs. It is, however, important to note that the formation of dead times in the SCU is actually a rather complex process because of the internal timing sequence in the PID-ADC circuitry and its implication for the event processing.

The PID circuitry is essentially a two-parameter analog PID with the ability to separate protons from heavier particles. Figure 5 is a representation of the E-T plane with measured proton and helium traces (borders correspond approximately to 1% detection probability) and PID decision lines L_1 and L_2. The PID evaluation process is initiated by a T signal (T priority) and requires in general the presence of T and E signals.

The PID classification logic and the corresponding scientific counting rates (HVY and PRO) are listed in Table 4. It should be noted that the system ignores all "mass zero" particles; i.e., events with (E, T) values below L_1. Evaluation of incomplete event patterns such as (0, T) or (E, 0) depends on the trigger conditions defined by TRIG LOG (Fig. 4).

As described previously, the TRIG LOG circuitry determines the event type; i.e., it defines four different event groups [$(E \cdot T)$, $(E + T)$, E, T events]. The analog evaluation process in the PID provides an additional event filter function which is illustrated in Table 5 for the trigger condition (E · T).

Housekeeping and Scientific Rate Channels. In accordance with the selected trigger condition in TRIG LOG, the SCU characterizes each detected particle event by its complete

Table 3 SCU Parameters

Parameter	Value
E-ADC	
Range	0–1500 keV
Resolution	8 bit[a]
Conversion time	42 μs
T-ADC	
Range	0–200 ns
Resolution	10 bit
Conversion time	42 μs
T-*E*	
Coincidence window	1.2 μs
PID	
Decision time	1.5 μs

[a]10-bit ADC, in the SCU reduced to 8 bit by omitting the two LSBs.

E and/or T data word. This primary information is complemented by 1) counting pulses from important subunits in the SCU such as the TAC or PID (so-called scientific counting channels); and 2) analog and digital housekeeping information.

A complete list of the scientific counting channels is given in Table 6 together with respective dead times t_D. The counting pulses are accumulated in the counter array CTR ARR (shown in Fig. 4). The DPU samples CTR ARR every 256 ms with a duty cycle of 75% (the precise timing is described in Sec. III.B). The relatively fast scientific counting channels are useful to correct the slow E- and T-ADC channels (compare Table 3) should the event rate exceed 2000 s^{-1}.

The analog housekeeping data (seven channels sequentially digitized in the 8-bit HK ADC) and the digital contents of the CMD RPT register (a copy of the current command status in the command receiver CMD RCVR) are a data set that supports the scientific data interpretation and verifies the functional integrity of the instrument. Two HK data words are transmitted in each telemetry format (see Sec. III.B).

DPU commands received by the SCU are transferred to the status control unit (STATUS CTRL) for execution. Major functions of the STATUS CTRL are 1) charge sensitive amplifier (CSA) ON/OFF; 2) energy threshold HIGH/LOW (40 keV/15 keV); 3) PID ON/OFF; 4) E and T calibrator ON/OFF; 5) TAC range setting (180, 200, 220, 800, and 1000 ns); 6) MCP bias setting (0 V, 8 steps 1–4 kV); 7) TRIG LOG condition ($T \cdot E$, $T + E$, E, T); and 8) HK-MUX scan mode.

4. Power and Data Coupler

Communication with and supply of power for the high-voltage bubble requires couplers which can reliably bridge the isolating gap. A major objective was to develop coupler systems which minimize violation of the guiding principles for the MICS high-voltage system. The use of opto-couplers with vacuum transmission for digital communication and magnetic coupling for power transformation resulted in a "tight" high-voltage design.

The principle design of the optical data couplers is shown in Fig. 2. The six coupler elements are evenly spaced on an annular structure. The active parts (phototransistor and light diodes) are recessed in the respective structure and only rather small holes in the isopotential surfaces are required for transmission across the vacuum gap. Design details of the mount ensure that sufficient shielding is achieved.

The power coupler, on the other hand, is much more complex. The principle of magnetic transformation obviously contradicts essential requirements for high-voltage isolation, high-conversion efficiency, electrostatic shielding, and confinement. As shown in Fig. 2, the power coupler is located at the backside of MICS in the axis of the dual bubble configuration. The coupler is part of the mechanical suspension and electrical isolation system for the inner bubble. Mechanically, the coupler is a body of rotation manufactured from a high-quality plastic specifically designed to transfer the necessary axial and lateral forces to the inner bubble. The outer surface is carefully shaped as a high-voltage standoff. On the inside two recessed volumes accommodate the transformer cores. Both sides of the plastic body are metallized to close the isopotential surfaces of the concentric bubbles.

As schematically shown in the block diagram of Fig. 4, the primary or ground side of the coupler operates from the 28-V line supplied by the DPU. The input circuitry regulates the voltage, limits the primary current with a turning characteristic, and provides a 90-kHz waveform for transformation. The current on the 28-V line is monitored and multiplexed into the housekeeping data stream.

On the secondary or high-potential side, the transformer is followed by a rectifying and regulating circuit to generate the necessary low voltages for the SCU electronics and the 100-V bias voltage for the SSD. The power coupler provides a total of 1.8 W for the SCU with an overall efficiency of about 70%.

Table 4 PID logic and scientific counting rates

Logic	Species	Scientific rate	ADC function
$\overline{L_1}\overline{L_2}$	Mass zero	—	0
$L_1\overline{L_2}$	Proton	PRO	0
L_1L_2	Helium or heavy particle	HVY	1

B. Digital Processing Unit and Data Structure

The DPU of the MICS spectrometer is in complete command of the SCU and the sensor system. The unit also accepts

Table 5 Effect of the PID circuit on scientific counting channels and ADC function for the trigger condition ($E \cdot T$)[a]

PID status	Event type		Scientific rates STA	DCR	TCR	ENY	PID rates PRO	HVY	ADC E	T
	E	0	—	—	—	+	—	—	—	—
							$18 \le T \le 38$	—	—	—
	0	T	+	+	—	—	—	$T \ge 38$	—	—
ON							—	—	—	—
							+	—	—	—
	E	T	+	+	+	+	—	+	YES	YES
							—	—	—	—
	E	0	—	—	—	+	—	—	—	—
OFF	0	T	+	+	—	—	—	+	—	—
	E	T	+	+	+	+	—	+	YES	YES

[a]Incremented accumulators are marked with a " + ".

Table 6 Definition of the scientific counting channels formed in the SCU and associated dead times t_D (duty cycle see Sec. III.B)

Code	Channel name/Source	t_D, μs
STA	(START)/TAC	4
TIM	(Time)/TAC	4
TCR	(E-T coincidence)/TRIG LOG	4
ENY	(Energy)/E-DISCR	2
PRO	(Proton pulse)/PID	4[a]
HVY	(Alpha pulse)/PID	4

[a]Dead time for protons, no heavy particle present.

the data outputs of the SCU (direct events, counting channels, and HK data), extracts particle parameters, and transforms the data into a format which is compatible with the telemetry system of CRRES. The following is a brief description of essential principles used to identify particle species and to organize the information transmitted to the ground. A detailed account of the DPU and its functions is given in Ref. 3.

The SCU in the MICS spectrometer converts each incident particle event into a binary 8-bit (E) and 10-bit (T) dual address. This primary particle information is transmitted to the DPU over a serial interface for selection and conversion in the MICS event processor:

1) Some of the events are sampled as so-called direct events (DE) for immediate transmission to the ground. These DE events are specified by a priority scheme. The DPU determines for each DE event the corresponding energy per charge step E/Q. After omitting the least significant bit (LSB) in the E and T words, a DE event is represented as (E, T, E/Q) = (7, 9, and 5 bit). A maximum of six DE events can be captured per 256 ms (this corresponds to the duration of a format as explained in the following).

2) Most of the detected (E, T) events are converted in a mass A and mass per charge A/Q classification process in order to reduce the bit stream to a tolerable level. The PID function is generated by constructing mass (or mass per charge) bins in (E, T) space. Decision boundaries are represented by polynomials of the form

$$\log T = c_0 + c_1 x + c_2 x^2 + c_3 x^3$$

where x represents log E or log(E/Q), respectively. A pair of polynomials is used to define upper and lower bounds for a mass A or a mass per charge A/Q species. The sets of coefficients are stored in the DPU. Following an instrument ON command, the DPU generates look-up tables (LUT) by evaluating the polynomials. Individual (E, T) events are then converted into (A, A/Q) pairs with reduced word length by using the LUTs. This approach achieves faster processing than direct computation of the particle parameter. The (A, A/Q) data pairs are accumulated in a A, A/Q scaler matrix. Eight selectable matrix elements or scaler Ri (i = 1-7) can be read out with high time resolution (see the following), whereas the complete matrix is transmitted with a much lower duty cycle.

The data acquisition and organization in the DPU is using multiples of a fundamental 32-ms time interval (frame), eight such frames represent a data format of 256-ms duration. In normal operations, the DPU sweeps in a preprogrammed sequence through the 32 voltage steps of the electrostatic analyzer with 256-ms (or one format) dwell time per step as illustrated in Fig. 6.

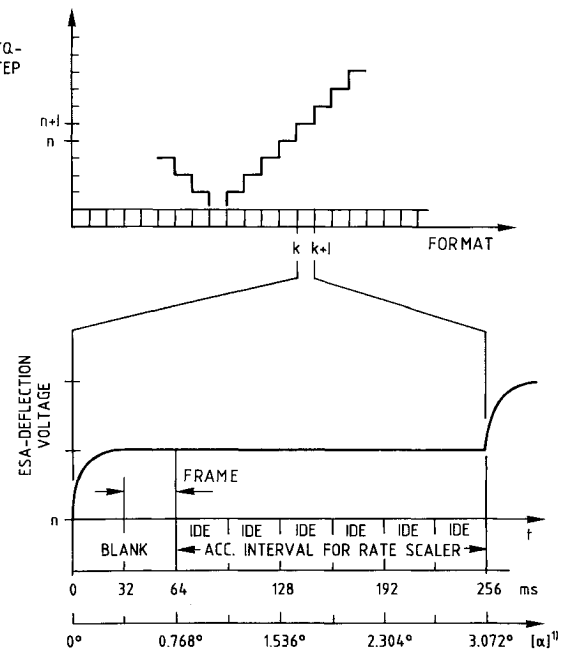

Fig. 6 Timing diagram for the DPU data acquisition.

Two stepping patterns, the normal mode and the auroral mode, are stored in the DPU. Both modes employ accelerated cycle times to increase time resolution.

1. Normal Mode

Semisymmetric triangular profile in 16 steps (duration 4096 ms) between lowest and highest level (full range).

2. Auroral Mode

Asymmetric sawtooth profile in eight steps (duration 2048 ms) between lowest level and a maximum level at 72.4 keV/e (reduced range).

In both modes consecutive cycles are not identical; the cycle repeat period is 32 steps for the normal mode and 16 steps for the auroral mode.

As indicated in Fig. 6, the DPU blanks all data for the first 64 ms (or two frames) of a format to allow the deflection voltage in the ESA to settle at the desired level. The remaining 192 ms are used as accumulation time for 1) the sixfold counter array CTR ARR in the SCU (scientific counting channels); 2) the eight rate scalers Ri in the DPU [(A,A/Q) matrix]; and 3) up to six DE.

Effectively the DPU sampling scheme creates an azimuthal sectoring which is synchronized with the telemetry clock. The azimuthal direction of incidence of a particle is determined from the time of observation in reference to the SEE SUN pulse. With a nominal spin period of T = 30 s, the duration of a format corresponds to an angular interval of $\Delta\alpha$ = 3 deg, which matches the angular opening of the instrument (2.2 deg). The azimuthal position of an individual DE is known to approximately ± 0.2 deg.

IV. Summary and First In-Flight Data

The MICS is an advanced time-of-flight/energy spectrometer with post-acceleration. The useful energy range extends from 430 keV/e down to about 1 keV/e. Ion species are identified from the function $M \sim (T^2 \cdot E)$. An electrostatic filter in front of the particle detection system accepts only particles within a preselected narrow energy per charge E/Q passband. The ionic charge state Q follows then from the energy measurement and the E/Q knowledge.

The time-of-flight/energy detector geometry is matched to an electrostatic analyzer of an unusual ogive design to achieve high system sensitivity coupled with a rather narrow collimation angle of ± 1.1 deg. MICS is therefore particularly suited to characterize the velocity distribution of dominant and minor species in the magnetospheric plasma with high angular resolution. MICS observations will play a major role in studies of dynamic processes in the magnetosphere and their coupling to the ionosphere and the solar wind. Direct or indirect plasma effects of the chemical release campaigns are also a major focus for MICS.

The instrument response function to incident ions and background radiation was carefully established during extensive ground tests. The forward sensitivity was characterized for a variety of ion species in the MPAe ion beam facility. The double and triple coincidence technique used in the PID process provides obviously inherent immunity to background. However, substantial fluxes of energetic electrons in the magnetosphere can lead to random coincidences. Passive shielding around the MICS sensor elements is employed to isolate the detectors from background radiation. Inspection of data returned from orbit shows that MICS tolerates background from relativistic electrons over most of the orbit.

The in-flight performance of MICS is illustrated by E/Q spectrograms for selected ion species shown in Fig. 7. The

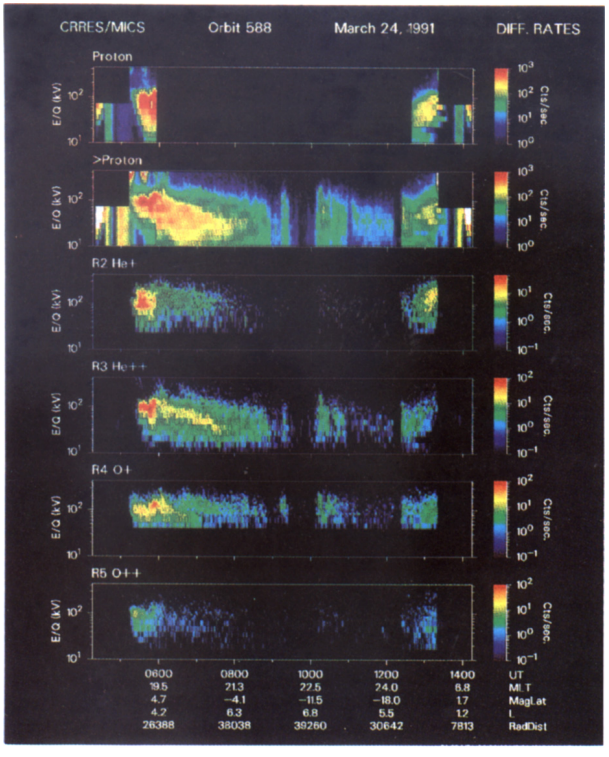

Fig. 7 Energy per charge spectrograms for major magnetospheric ions. The observations were obtained shortly after the onset of a large storm. Strong injections of solar wind ions ($He^{+\,+}$) and ionospheric ions (O^{+} and $O^{+\,+}$) are detected at 0530 UT. The upper two panels are the PID rates PRO and HVY.

measurements are obtained after the onset of a strong magnetic storm during the preceding orbit.

The upper two panels are constructed from the two PID channels (PRO and HVY, see Table 5). At low altitudes (at the beginning and end of the pass), the PID circuit was in the ON state to eliminate high proton rates from the digitization process. For these time periods (before 0600 UT and after 1230 UT), the PRO channel (marked as proton in Fig. 7) responds to all events identified by PID as protons and the HVY channel counts all ion species except those recognized as protons. At 0600 UT PID was commanded OFF. In this condition the PRO channel is inhibited as can be seen in the top panel. The HVY channel, however, accepts all events with a valid time-of-flight T; i.e., the HVY rate now represents all ion species including protons. At 1230 UT PID is again activated for the low altitude leg of the orbit and the data are again in the nominal format.

The lower four panels in Fig. 7 show spectrograms for the species He^{+}, He^{2+}, O^{+}, and O^{2+} which were identified by the DPU classification process. As can be seen, the storm has obviously injected substantial fluxes of ionospheric particles (O^{+} and O^{2+}) and particles of solar wind origin (H^{2+}). The oxygen ions seem to be concentrated at relatively low L values ($L \approx 4$), whereas the solar wind alpha particles populate the magnetosphere also at larger radial distances (out to about $L \approx 6.5$).

Acknowledgments

The MICS spectrometer was designed and constructed with support from the Max-Planck-Gesellschaft zur Förderung der Wissenschaften. Grants were received from the USAF Office of Scientific Research under AFOSR 85-0237 (MPAe and RAL) and from the Norwegian Research Council for Science and the Humanities to the University of Bergen. The data processing unit and instrument integration were supported at the Aerospace Corporation under Air Force Space Systems Division Contract F 04701-88-C-0089.

The MICS/CRRES signal conditioning unit was designed by the MPAe and jointly manufactured together with the University of Bergen (UoB), Bergen, Norway. Design and production of the toroidal analyzer and the high-voltage generators (VVPS and HVPS) were contributions of the Rutherford-Appleton Labs. (RAL), Oxford, England, UK. The Aerospace Corporation (AC), Los Angeles, assumed responsibility for the DPU design, fabrication, and software development including verification of the onboard sorting process. Production of the detector system, assembly of the MICS unit, electronic characterization and beam calibration of the spectrometer was in the authority of MPAe. The MICS-CRRES experimenter team truly acknowledges the technical and engineering assistance and support received from S. Njaastad and A. Solberg (both UoB), K.-H. Otto, H. Sommer, and H. Wirbs (all MPAe), K. Slater (RAL), and N. Katz, S. Imamoto, S. Pinkerton (all AC). We also would like to express our thanks to Meier-Komor, Technische Universität, München, for the provision of high-quality carbon foils for the time-of-flight spectrometer. We are also indebted to P. Lew (AC) for the preparation of the real-time quick look plots.

References

[1]Wilken, B., "Identification Techniques for Nuclear Particles in Space Plasma Research and Selected Experimental Results," *Report on Progress in Physics,*, Vol. 47, No. 7, 1984, pp. 767–853.

[2]Gough, P., Ph.D. Thesis, Univ. of Southampton, Southampton, England, UK, 1982.

[3]Koga, R., Imamoto, S. S., Katz, N., and Pinkerton, S. D., "Data Processing Units for Eight Magnetospheric Particle and Field Sensors," *Journal of Spacecraft and Rockets,* Vol. 29, No. 4, 1992, pp. 574–579.